

UDC 621.4

doi: 10.32620/akt.2025.1.02

Pavlo GAKAL, Igor RYBALCHENKO, Oleksii TRETIAK, Viacheslav NAZARENKO

National Aerospace University “Kharkiv Aviation Institute”, Kharkiv, Ukraine

EXPERIMENTAL INVESTIGATION OF THE PERFORMANCE OF A LOOP HEAT PIPE-BASED COOLING SYSTEM UNDER ULTRA-HIGH BYPASS RATIO TURBOJET ENGINE CONDITIONS

The subject of this article is the heat transfer processes in a loop heat pipe (LHP) to solve the problem of maintaining the temperature regime of the valves of the air-bleeding system of an aircraft engine. The goal was to experimentally substantiate the operability and efficiency of a cooling system based on LHP for the temperature conditions of a perspective aircraft engine with an ultra-high bypass ratio. The task to be solved: to create a test bench for studying heat transfer processes in cooling systems based on LHP. The test bench should reproduce the temperature of the aircraft engine and the orientation of the LHP in the gravitational field. To investigate the operability of the cooling system under different heat loads, heat sink temperatures, orientation in the gravitational field, and additional thermal insulation. The methods used are: experimental approach, test planning, and statistical methods for processing experimental results. The following results were obtained. A test bench was created to investigate the heat transfer processes in a cooling system based on LHP. Toluene is used as a LHP's coolant. The temperature conditions of the perspective aircraft engine were considered when creating the test bench. The performance of the cooling system was studied under different orientations of the gravitational field, heat sink temperature, and heat load. The obtained experimental results allowed us to analyze the influence of the orientation in the gravitational field, heat sink temperature, and additional vacuum thermal insulation of the evaporator and liquid line on the LHP performance and efficiency. Conclusions. The novelty of the results obtained is as follows: for the first time, the possibility of using a cooling system based on the LHP in temperature conditions of the perspective aircraft engine with an ultra-high bypass ratio was experimentally approved; it was proven that the LHP with toluene as part of the cooling system can effectively operate stably, without pulsations and without overheating of the cooled devices under different heat loads, heat sink temperatures, and orientation in the gravitational field.

Keywords: cooling system; loop heat pipe; heat transfer; turbojet engine with ultra-high bypass ratio; fuel consumption.

1. Introduction

Motivation of work.

A new generation of turbojet aircraft engines with ultra-high bypass ratio (UHBR) will surpass existing engines in technical, operational and environmental performance, particularly, in term of reduced fuel consumption and, consequently, CO₂ emissions. However, the UHBR engine components will operate in harsher temperature conditions due to the increased compression ratio and gas temperature upstream of the turbine. The more sensitive to the increased temperature are the valves of engine bleed system. In current turbojet aircraft engines, the valves of bleed air system are not specially cooled. Instead, they rely on the so-called “engine compartment air” for cooling. But, in new generation of UHBR engines, the temperature of the air in the engine compartment can reach 300°C and, as a result, no longer providing the necessary cooling of the bleed system valves. Additionally, it is important to consider that the sole ‘cold sink’ of the engine is the

secondary airflow, which can reach temperatures of up to 100°C. Therefore, a specialized cooling system is necessary to remove heat from the valves and ensure their temperatures within the specified limits (no more 200°C).

Nowadays, the most effective thermal management systems are based on the two-phase passive heat transfer devices, namely heat pipes (HP) and Loop Heat Pipes (LHP). Now these devices are widely used in spacecraft [1, 2] and terrestrial applications.

State of the art.

In the aircraft engines, LHPs are not yet widely employed. Therefore, we will review only the articles that consider the general issues of using HP and LHP in aviation. In the review, we will pay attention to the temperature conditions of the HP and LHP operation. In particular, the ambient temperature and the heat sink temperature.

The initial attempts to use LHP in aircraft anti-icing systems began in the early 2000s. The results obtained during this period are presented in [3] and [4]. In [3] a



passive anti-icing system for the engine cowl of Global Hawk is described. Five LHPs were utilized, successfully removing 3.8 kW of the waste heat from the hydraulic system during the icing conditions. Ammonia was used as a working fluid. The nickel cylindrical wick with a pore size 0.9 μm was implemented in the LHP evaporator. According to the authors, the anti-ice system effectively provided ice protection for the engine inlet and could be feasibly installed on real aircraft.

Other recent works relevant to the use of LHPs in anti-icing systems include [5] and [6]. In [5], the heat transfer performance of a stainless steel-nickel loop heat pipe was investigated. To address the freezing issues under negative temperature flight conditions, an ethanol-water mixture with varying concentration was used. The operational temperatures ranged from 70°C to 100°C, and heat load ranged from 100 W to 300 W. In the considered systems, the maximum temperature did not exceed 100 °C, and the heat was removed to an environment with a temperature below 50 °C.

The work [6] focuses on reviewing LHPs for aircraft anti-icing and presents fundamental as well as optimized designs along with specific technological guidance. In the context of anti-icing on aircraft, various potential heat sources exist, for example: the engine oil, the low/high pressure compressor bleed air, the hot turbine case, hydraulic system and exhaust gases in the nozzle. Their corresponding temperatures are listed below in the Table 1:

Table 1
Temperature of heat sources

Heat source	Temperature, °C
Air/Oil cooler	130
Low pressure compressor bleed air	100
High pressure compressor bleed air	260
Turbine case	430
Exhaust nozzle	415
Hydraulic system	160...165

The experimental studies on the key aspects of the LHP ice-protecting system are also summarized in this paper. The main conclusions drawn from these experimental studies are as follows:

- more preferable working fluids – Methanol, Ethanol, Toluene, Ammonia, Water, Acetone;
- operation temperature range – 10...80 °C;
- heat transfer capacity – 100...1500 W.

The experimental investigation of the start-up and operating characteristics of the Double Compensation Chamber Loop Heat Pipe for anti-icing system is also presented in [7]. The LHP was made of stainless steel with nickel wick, and ethanol was used as the working fluid. Experiments were conducted with heat loads

ranging from 10 W to 180 W. The primary emphasis in the paper was on studying the impact of the attack angle and start-up time.

The short description of the LHP design investigations for aircraft anti-icing is also outlined in [8]. As the authors highlight, a significant limitation in the past for LHPs using in the aircraft anti-icing system was the achievable pressure head by the capillary action wick. However, recent advancements in wick materials have demonstrated a drastic increase in achievable pressure head of the LHP. This increase is estimated to extend the working distance of LHP from the current 8–10 m to 28–35 m.

The paper [9] focuses on in-flight tests of the passive cooling system utilizing heat pipe technology. The system employed a heat pipe as intermediary heat transfer element between the airplane's equipment and the main heat exchanger system. Water was applied as the working fluid. The input power ranged from 40 W to 120 W, and the temperatures were within the range of 20 to 80°C. The heat pipe thermal resistance, R_{HP} , was measured at 0.33 K/W with an input power of 120 W, while the condenser temperature was only approximately 30 °C.

Aiming to enhance avionics cooling, a specialized LHP with high heat transfer capacity is described in [10]. The paper provides comprehensive details on the design criteria, the entire design process, including the justification for working fluids. Moreover, it encompasses an extensive experimental validation, covering startup, steady state, and dynamic operation performance of the LHP, effectively confirming the accuracy of the proposed design approach. Based on the design process and experimental findings, several key conclusions have been drawn:

- ammonia should be the optimal working fluid for LHP technology applied in avionics cooling considering the operating temperature range, heat transfer capacity, and adaptation to large acceleration;
- it is ideal to prioritize the flow resistance in the capillary wick as the primary resistance, which can minimize the influence of pipeline arrangements and effectively enhance the heat transfer capacity of the LHP to kW-level;
- the designed LHP demonstrates a kW-class heat transfer capacity of 1021 W, corresponding to an average heat flux of 12.04 W/cm² at the evaporator, with maximum saddle surface and vapor temperatures of 88.8 °C and 52.6 °C, respectively.

Among the works devoted to the issues of cooling electronic devices on board an aircraft, work [11] should be noted. However, thermosyphons are used as passive heat transfer devices. The paper [12] presents the experimental assessment of an electronic cooling prototype especially designed for helicopter avionics

thermal management. The prototype consists of a set of LHPs especially designed for the hot spot treatment at electronic blade level and a cooled mini-Vapour Cycle System, which is devoted to the overall heat rejection. The experimental results are carried out at different heat loads from 10 W to 50 W. The ambient temperature was 70 - 85°C. The effect of different heat sink temperatures on the LHP thermal resistance is investigated. The tests showed that the architecture is worth of future research investigation for proper integration in avionics cooling strategies. This new cooling technology offers promising performances, above state of the art with up to 55°C benefit at 40 W as compared to classical cooling system.

The paper [13] is devoted to the passive thermal energy transport from the aircraft electronics enclosure to selected sinks. The system developed to accomplish these tasks is divided into two subsystems. The first subsystem is responsible for improving thermal transport within the electronics enclosure and consists primarily of heat pipe assemblies. Model results of the first subsystem show considerable improvements over the current implementation. The overall temperature gradient within a generic electronics box decreased from 42.7°C to 17.8°C, increasing the allowable sink temperature from 66.7°C to 91.7°C. The second subsystem transports thermal energy from the external surface of the enclosure to appropriate sinks and consists primarily of the LHP. Depending on sink temperature and capacity throughout the operating envelope of the platform, multiple sinks may be used. During operation, the LHP will passively select the appropriate sink.

Among the latest articles that discuss the use of LHP for cooling electronic components in avionics, the article [14] should be mentioned. The experimental investigation of LHPs used in the cooling system is described in this article. The proposed LHPs allow transferring up to 40 W over a distance of approximately 100 mm at an operating temperature 20°C only.

The paper [15] addresses the thermal management of electromechanical flight control actuators on an all-electric aircraft. Several thermal management system concepts, including the concept with flexible heat pipes, were identified, and the best of these concepts were evaluated based on their application to a case study aircraft. The main conclusion is that detailed design, simulation and testing of hardware will ultimately be required to determine which system offers the best solution for the case study application.

The system with LHPs that allow free-energy heat transportation between certain subsystems without needing additional power consumption is presented in [16]. Their use in aeronautics is interesting as they can passively transport seemingly “waste” heat to areas where it can be reused.

The objective of work and using approach.

Based on the review it is evident that the LHPs described above have a maximum working temperature of no more than 100°C. The impact of high surrounding temperatures on LHP functionality and performances has not been adequately addressed. However, as mentioned earlier, in the new generation UHBR engines, the air temperature in the engine compartment - where the LHP is located - can reach up to 300°C. Additionally, the heat sink temperature exceeds 100°C. In the reviewed articles, these temperatures are either significantly lower or not mentioned at all. Furthermore, not enough attention has been given to analyzing the influence of LHP orientation in the gravity field.

Therefore, the objective of this study is to conduct the experimental confirmation of LHP functionality under harsh surrounding air temperature conditions, as well as to analyze the influence of the heat sink temperature, heat load, thermal insulation of LHP components and LHP orientation in the gravitation field on its operability and heat transfer performances.

2. LHP design description

The LHP principal scheme also as LHP Evaporator Block are presented into Fig. 1. The LHP was established with using ALTOM design [17]. The main elements of LHP were:

- Heater;
- Evaporator block located in the vacuum insulation box;
- Vapour line;
- Liquid line;
- Condenser mounted on an aluminum cold plate.

The evaporator block included two capillary pumps and three compensation chambers. The liquid manifolds provided the connection between capillary pumps and compensation chambers. The evaporator block and liquid line had the possibilities to minimize the additional heat load from the hot surrounding air. For this reason, the evaporator block was enveloped in the vacuum insulation box. Liquid line was also enveloped in the external concentric tube, and the gap between internal and external tubes had possibility to be vacuumed too.

The wick had the cylindrical shape and was made of sintered in vacuum stainless-steel powder and fiber mixture. In general, the Table 2 presents the basic parameters of the LHP components. In Table 2, OD and ID represent the outer and inner diameters respectively, CC represents the compensation chamber. Toluene was selected as the working fluid due to its good thermophysical properties for the temperature over 100 °C [18].

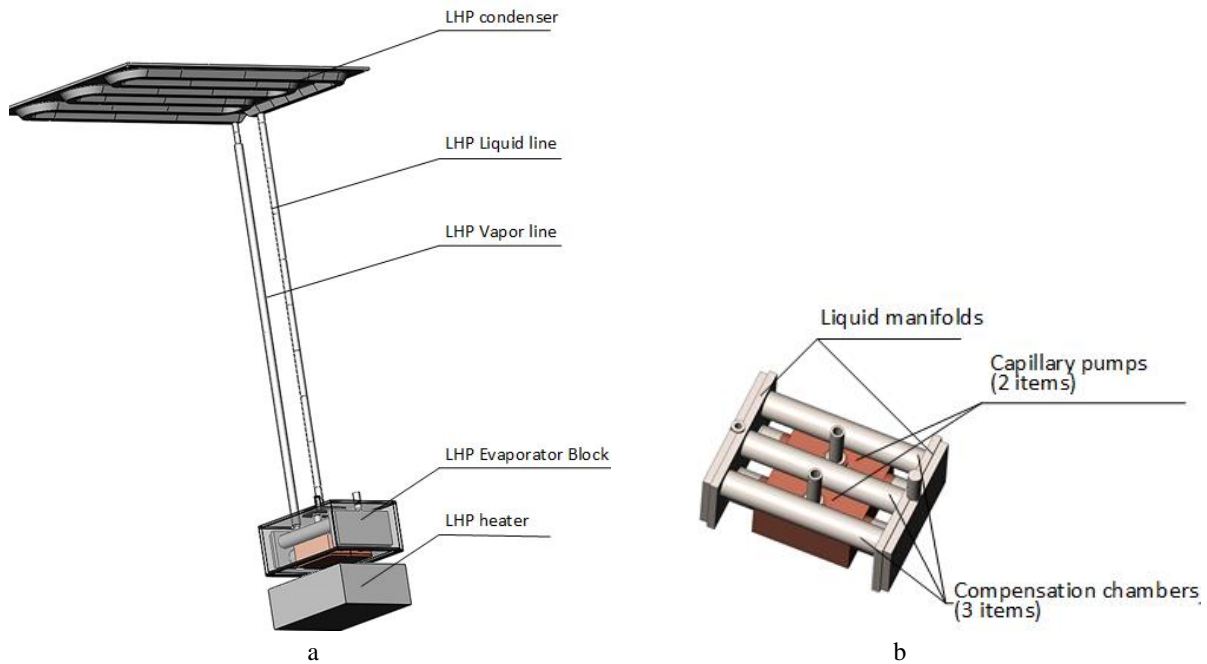


Fig. 1. LHP and LHP evaporator block principal views:
 a – LHP;
 b – Evaporator block

Table 2

The basic parameters of the LHP components

Component	Parameter	Value
Vapor line	O.D.×I.D.×Length	5×4×300 mm. Stainless steel tube
Liquid line (internal tube)	O.D.×I.D.×Length	3×2×300 mm. Stainless steel tube
Liquid line (external tube)	O.D.×I.D.×Length	5×4×300 mm. Stainless steel tube
Condenser	O.D.×I.D.×Length	5×4×1315 mm. Stainless steel tube mounted on the aluminum cold plate
Wick	Shape	Cylindrical
	Material	Sintered in vacuum stainless-steel powder and fiber mixture
	I.D./O.D./Length	5.5 mm/10.6 mm/50 mm
	Porosity	0.45
	Permeability	$1.48 \times 10^{-13} \text{ m}^2$
Radius of capillary pores		1 μm
CC	Number×Volume	3×3.6 mL. Stainless steel tube
Charge of working fluid at 20°C	Volume	25 mL

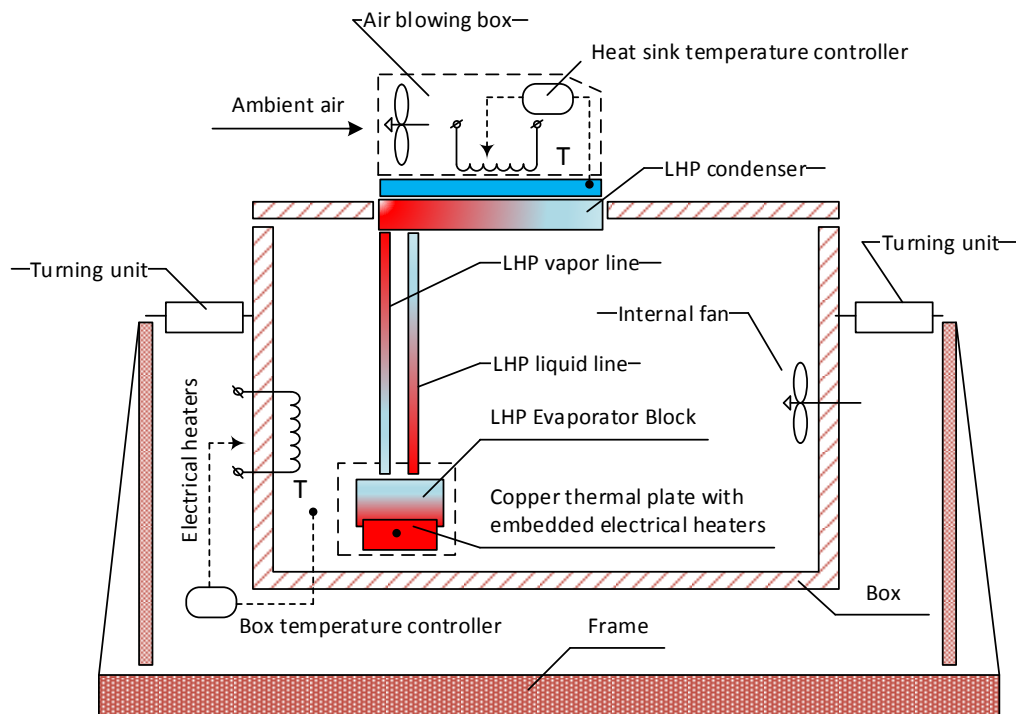


Fig. 2. Principal scheme of Test bench

3. Test bench description

The test bench allows to simulate the heat sink temperature (the temperature of the engine secondary air flow) T_{sink} , the surrounding temperature (engine compartment temperature) around the loop heat pipe T_{box} and the orientation of the LHP in the gravity field. The principal scheme of Test bench is shown in Fig. 2.

The Test bench includes:

- LHP;
- Frame with the turning units;
- Box;
- Air blowing box.

A frame with turning units was utilized to hold and secure the box. The box could be rotated within the range of 0° to 180° to simulate the gravity effect. The box was established to simulate the temperature conditions of the engine compartment. Temperature inside the box T_{box} was controlled by the three electric heaters. An internal fan was used to ensure a uniform temperature field within the box.

For simulating the heat sink temperature T_{sink} (representing the air temperature in the engine secondary flow), an air blowing box was used. The external surface of the LHP condenser was located on a copper thermal plate with an embedded electrical heater (Fig. 3). An additional radiator was used to enhance heat rejection to the

ambient air. The heat sink temperature T_{sink} was simulated by maintaining a required temperature of the copper thermal plate. Cylindrical electrical heaters embedded in the copper thermal plate provided heat load Q_{evap} applied to the LHP evaporator block. The heat load can be adjusted from 0 W to 150 W by altering the output voltage of the DC power. The temperature of surface between copper thermal plate and LHP evaporator block T_{surf} was used for the LHP efficiency analysis. The data acquisition system was composed of a data logger linked to a PC and the LabView software, which was used to display and store the experimental data. Chromel/Alumel (Type K) thermocouples (TCs) were used to measure the temperatures along the loop. In the experiment, the maximum measurement error of the thermocouples was ± 0.5 C, and the uncertainty of the

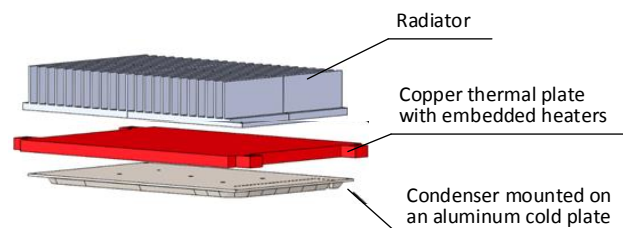


Fig. 3. LHP condenser with copper thermal plate and radiator

heat load applied to the evaporator was within 1.2 % in the full range.

4. Experimental conditions and procedure

The surrounding air temperature conditions with the temperature $T_{\text{box}} = 300^{\circ}\text{C}$ was only considered. The tests were conducted in two cases: one without vacuum insulation for the liquid line and evaporator block, and the other with vacuum insulation for these parts. The heat sink temperature T_{sink} and LHP heat load Q_{evap} were:

- the heat sink temperature $T_{\text{sink}} - 100, 110, 120$ and 150°C ;
- LHP heat load $Q_{\text{evap}} - 25, 50, 75, 100, 125$ and 150 W
- three positions in the gravity field were also considered:
 - Vertical position (condenser on top) at $\varphi=0$ deg;
 - Horizontal position at $\varphi=90$ deg;
 - Inclined position (condenser down) at $\varphi=135$ deg.

All experimental cases are summarized in Table 3.

The following test procedure for each case was used:

- set the box T_{box} and heat sink T_{sink} temperatures and to wait for the steady state reaching;
- set the required value of heat load Q_{evap} ;
- waiting for the reaching of the steady state. For this, if the temperature variations were within $\pm 2^{\circ}\text{C}$ over a 10-minute period, it was considered that the LHP had reached a steady state. All parameters were then held constant, and the mean value for all temperatures and heat load was calculated during this period.

Effective thermal resistance R_{LHP} offered by a LHP from the evaporator to the condenser to be used to evaluate the heat transfer efficiency and this value was defined as:

$$R_{\text{LHP}} = \frac{T_{\text{surf}} - T_{\text{sink}}}{Q_{\text{evap}}}, \quad (1)$$

where T_{surf} is the temperature on the surface between copper thermal plate and LHP evaporator block.

5. Results and discussions

The change of the temperature T_{surf} when the LHP heat load Q_{evap} changing without and with vacuum thermal insulation and with different LHP orientations in the gravity field for cases 7 - 12 and 19 – 24 is depicted into the Fig. 4 and 5. For the remaining cases the situation are similar. These results illustrate that the LHP design employing ALTOM technology has demonstrated the stable operation and reliable heat removal behavior across the entire range of variations in Q_{evap} , T_{sink} and different LHP orientations within the gravitational field. This observation holds true for both cases with and without vacuum insulation. As follows from the presented results, when Q_{evap} changes, the temperature T_{surf} remains practically unchanged (Fig. 6). This conclusion is true for all values of the heat sink temperature T_{sink} , the presence or absence of additional thermal insulation, and orientation in the gravity field. For example, the most significant change in T_{surf} is observed at the temperature $T_{\text{sink}} = 110^{\circ}\text{C}$, vertical ($\varphi=0$ deg.) orientation (condenser at the top) and the absence of additional thermal insulation. In this case, T_{surf} changes only by about 10°C from $\sim 180^{\circ}\text{C}$ at $Q_{\text{evap}} = 25\text{ W}$ to $\sim 170^{\circ}\text{C}$ at $Q_{\text{evap}} = 150\text{ W}$. In other cases, the T_{surf} changing is even smaller. This can be explained by the fact that additional heat inflows to the LHP elements from the

Table 3
Experiment conditions

Case	Evaporator power Q_{evap} W	Orientation φ , degree	Heat sink temperature T_{sink} , $^{\circ}\text{C}$	Vacuum insulation
	Range; increment			
1	25 – 150; 25	0	100	No
2	25 – 150; 25	0	100	Yes
3	25 – 150; 25	90	100	No
4	25 – 150; 25	90	100	Yes
5	25 – 150; 25	135	100	No
6	25 – 150; 25	135	100	Yes
7	25 – 150; 25	0	110	No
8	25 – 150; 25	0	110	Yes
9	25 – 150; 25	90	110	No
10	25 – 150; 25	90	110	Yes
11	25 – 150; 25	135	110	No
12	25 – 150; 25	135	110	Yes
13	25 – 150; 25	0	120	No
14	25 – 150; 25	0	120	Yes
15	25 – 150; 25	90	120	No
16	25 – 150; 25	90	120	Yes
17	25 – 150; 25	135	120	No
18	25 – 150; 25	135	120	Yes
19	25 – 150; 25	0	150	No
20	25 – 150; 25	0	150	Yes
21	25 – 150; 25	90	150	No
22	25 – 150; 25	90	150	Yes
23	25 – 150; 25	135	150	No
24	25 – 150; 25	135	150	Yes

ambient air with a temperature of 300 °C significantly exceed Q_{evap} and, as a result, such a weak dependence of T_{surf} on Q_{evap} is observed.

Also, as follows from the presented results, the additional thermal insulation reduces the temperature T_{surf} . For instance, the surface temperature T_{surf} in the presence of thermal insulation decreases by

approximately 5...10 K compared to the case without thermal insulation. The most significant decrease is observed at $Q_{evap} < 75$ W. At $Q_{evap} \geq 75$ W, the effect of thermal insulation becomes insignificant. This can be explained by the fact that at $Q_{evap} \geq 75$ W, heat inflows from the ambient air become comparable both with and without thermal insulation. This trend is true for all values of T_{sink} and LHP orientation in the gravity field.

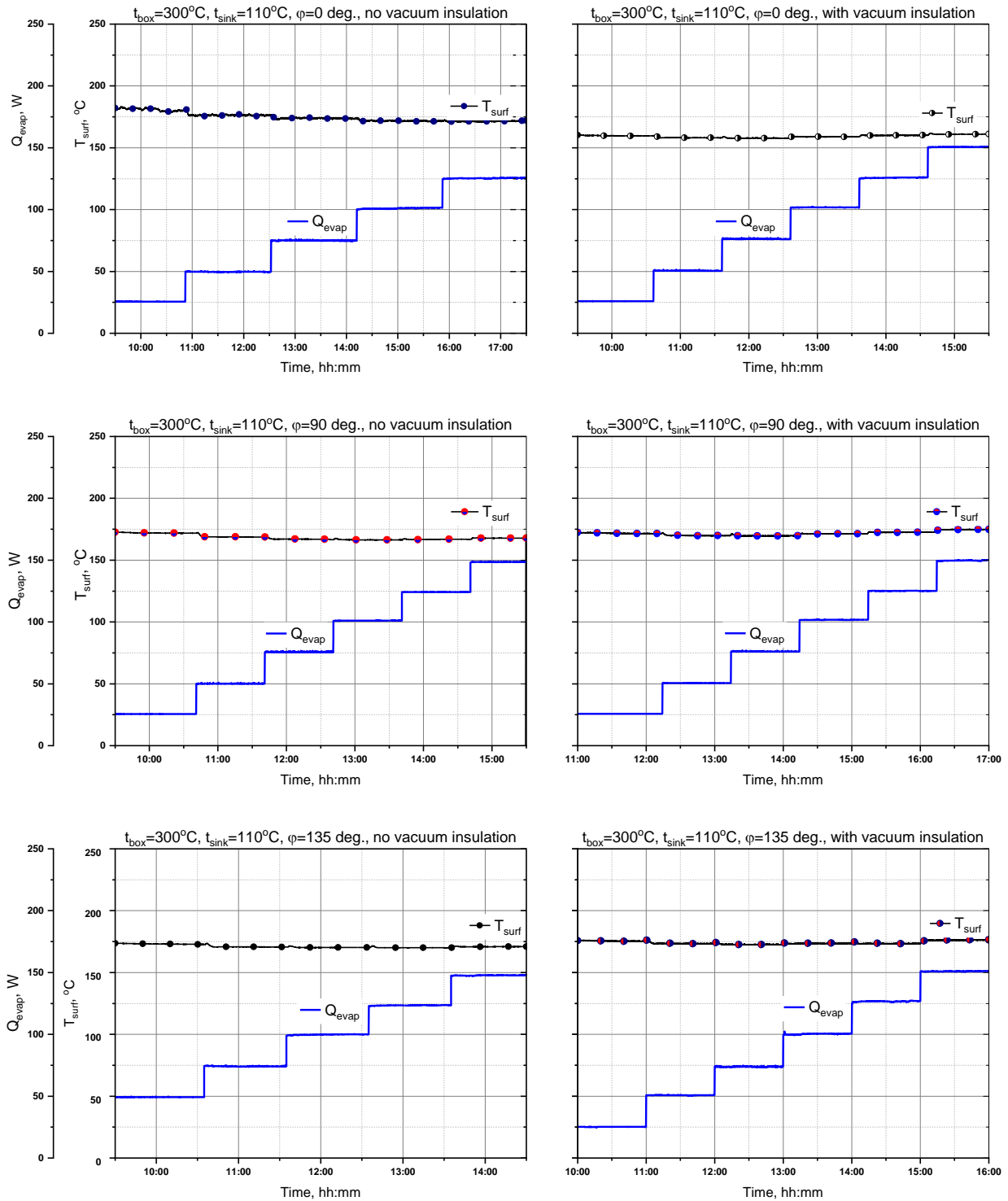


Fig. 4. Effect of heat load Q_{evap} on the surface temperature T_{surf} for cases 7–12 (see Table 3)

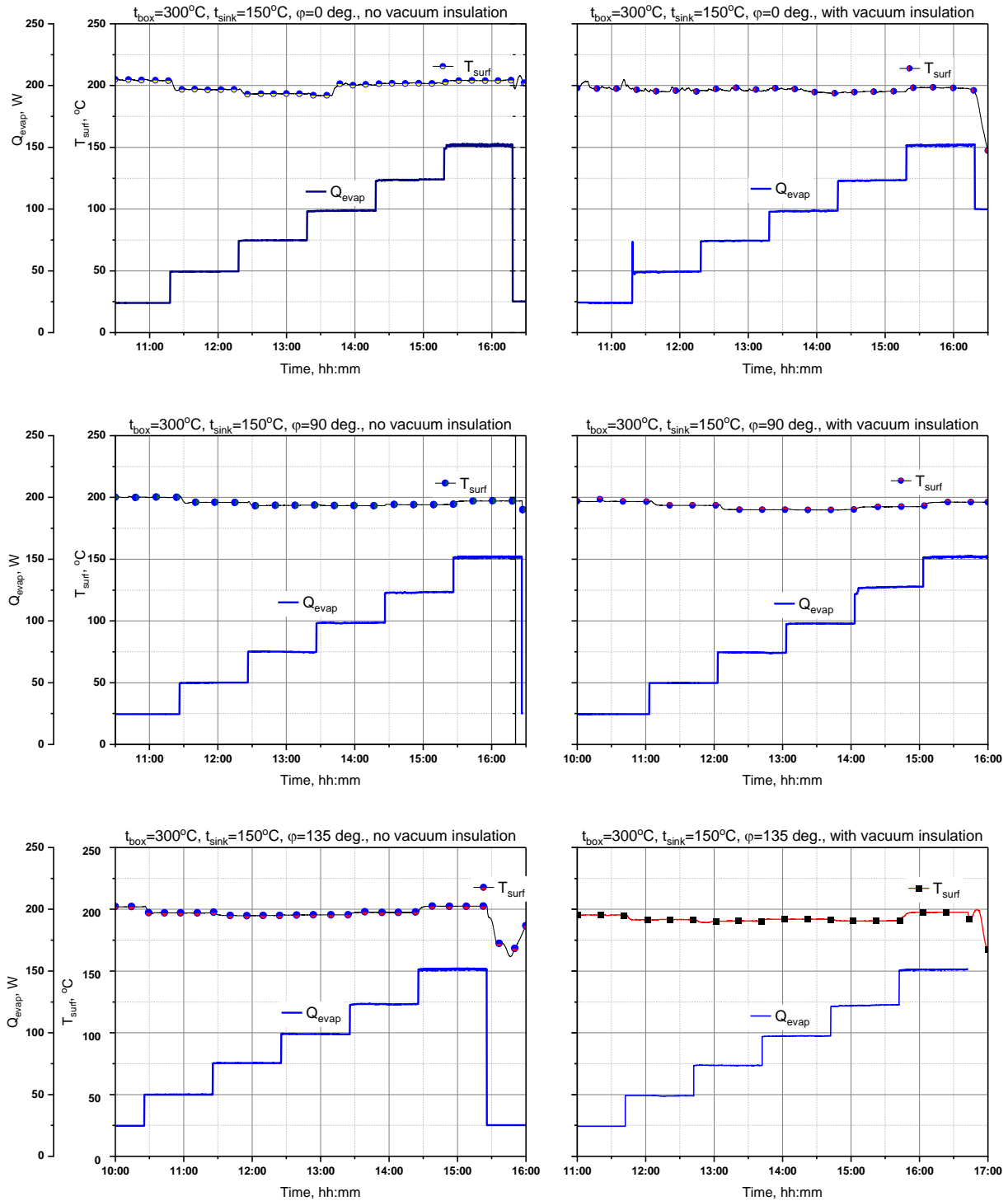


Fig. 5. Effect of heat load Q_{evap} on the surface temperature T_{surf} for cases 19–24 (see Table 3)

The effect of the heat sink temperature T_{sink} on the temperature T_{surf} is illustrated in Fig. 7. As follows from the data, with the T_{sink} increasing, the temperature T_{surf} increases almost linearly, and when T_{sink} increasing from 100 to 150 °C, the temperature T_{surf} increases by about 40 °C. That is, an almost direct linear dependence. This

conclusion is true for all LHP orientations in the gravity field, with or without thermal insulation. Such a dependence of T_{surf} on T_{sink} also shows that the thermal resistance of the LHP (see Eq.1) also weakly depends on T_{sink} and is in the range of $R_{LHP} = 0.4...3 \frac{\text{K}}{\text{W}}$.

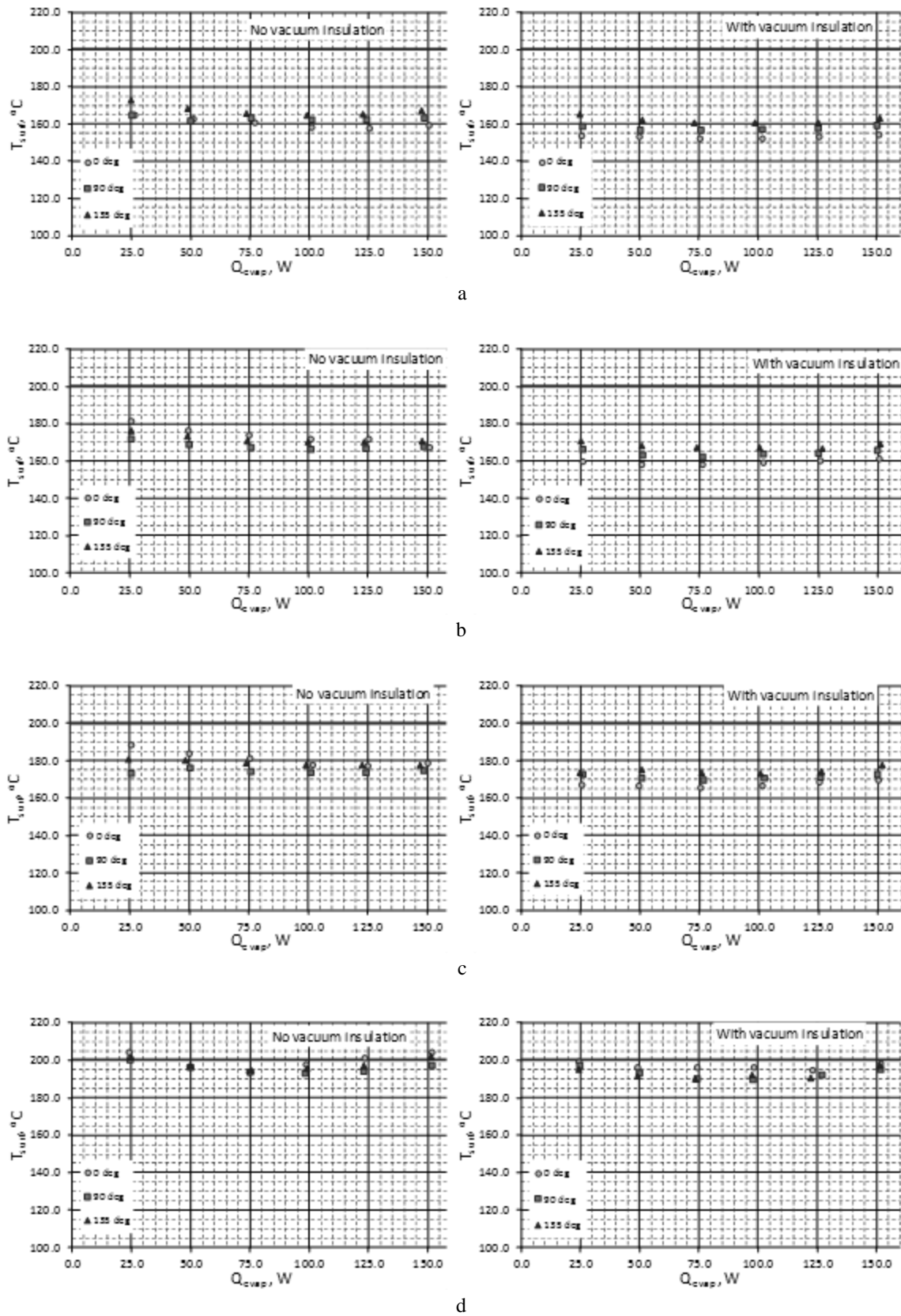


Fig. 6. LHP surface temperature T_{surf} versus LHP heat load without/with vacuum insulation and different orientation:
 a - $T_{sink} = 100^{\circ}C$; b - $T_{sink} = 110^{\circ}C$; c - $T_{sink} = 120^{\circ}C$; d - $T_{sink} = 150^{\circ}C$

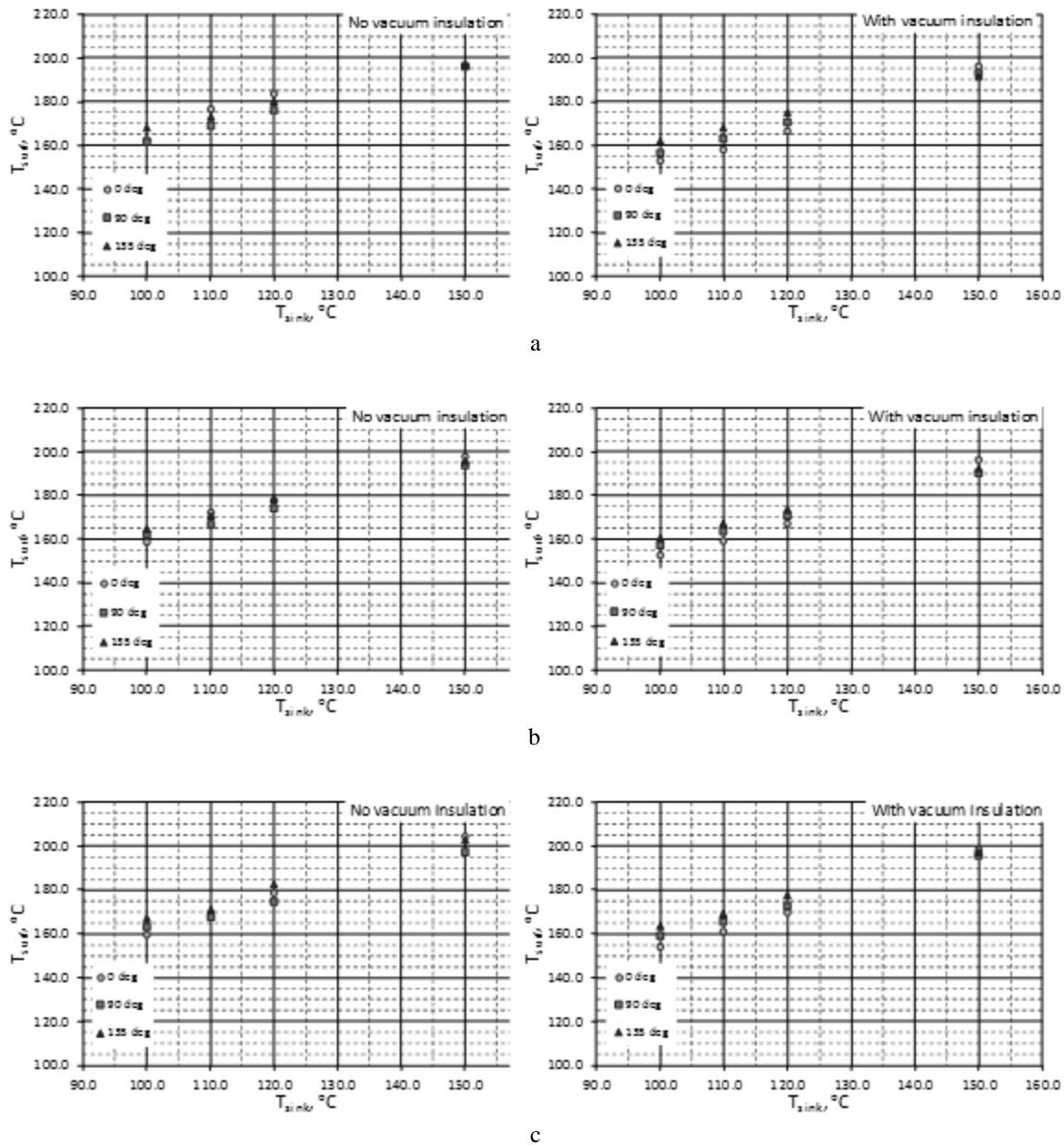


Fig. 7. LHP surface temperature T_{surf} versus heat sink temperature without/with vacuum insulation and different orientation:

a – $Q_{evap} = 25 \text{ W}$; b – $Q_{evap} = 100 \text{ W}$; c – $Q_{evap} = 150 \text{ W}$

As follows from the results presented in Fig. 6 and 7, the most significant effect of orientation is observed at $T_{sink} < 150^\circ\text{C}$. In addition, with Q_{evap} increasing, the effect of orientation weakens. This can be explained by the fact that with Q_{evap} increasing, the mass flow rate of toluene in the LHP increases and the hydrostatic pressure drop becomes insignificant compared to pressure losses due to friction and local resistances.

Based on the presented results it can be mentioned that the LHP performances is significantly affected by

additional heat inflows from the ambient air. It is impossible to quantitatively estimate these heat inflows based on the available experimental data. It can only be stated that this additional heat significantly exceeds Q_{evap} and the presence of additional thermal insulation of the evaporator and liquid pipeline has practically no effect on the value of these heat inflows.

The LHP thermal resistance versus LHP heat load Q_{evap} without/with vacuum insulation, different heat sink temperature T_{sink} and different orientation is depicted into Fig. 8.

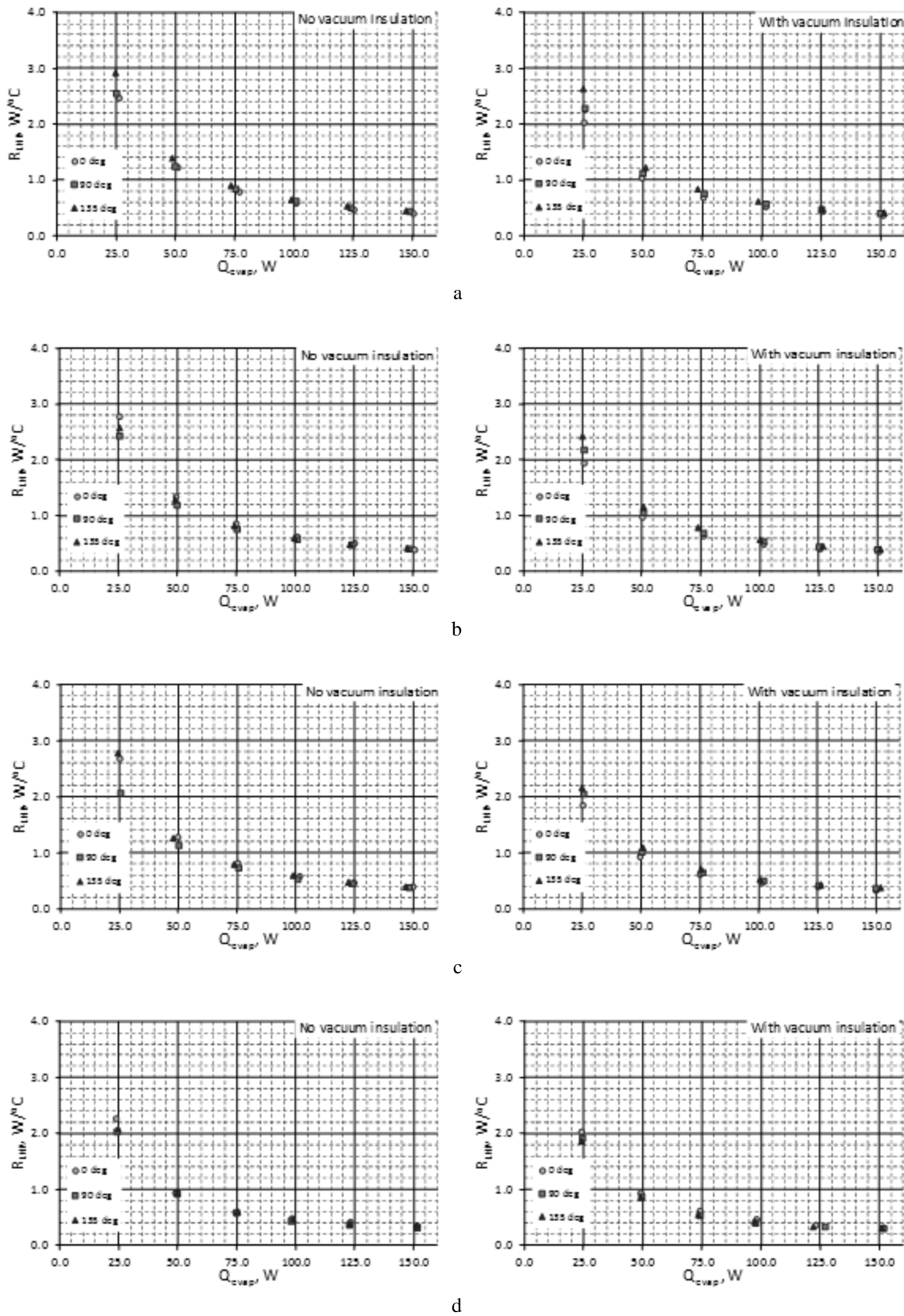


Fig. 8. LHP thermal resistance R_{LHP} versus LHP heat load without/with vacuum insulation and different orientation:
 a – $T_{\text{sink}} = 100^\circ\text{C}$; b – $T_{\text{sink}} = 110^\circ\text{C}$; c – $T_{\text{sink}} = 120^\circ\text{C}$; d – $T_{\text{sink}} = 150^\circ\text{C}$

6. Conclusions

In this paper, the LHP functionality and its thermal performance were experimentally studied. The LHP was designed using ALTOM technology, and toluene was employed as the working fluid. The investigations covered the following parameter ranges: air surrounding temperature at 300°C, heat sink temperature between 100°C and 150°C, and heat loads ranging from 25 W to 150 W. The study examined the impact of thermal (vacuum) insulation on the liquid line and evaporator, as well as the influence of LHP orientation in the gravity field. Based on the experimental results, the following conclusions are drawn:

1. LHP operates greatly without temperature oscillations and overshooting in the whole range of heat load Q_{evap} , heat sink temperature T_{sink} , orientation in gravity field, with and without thermal insulation.

2. The weak dependence of T_{surf} on Q_{evap} is observed. This can be explained by the fact that additional heat inflows to the LHP elements from the ambient air with a temperature of 300 °C significantly exceed Q_{evap} .

3. At $Q_{\text{evap}} \geq 75$ W, the influence of thermal insulation becomes insignificant for all values of T_{sink} and LHP orientation in the gravity field. This can be explained by the fact that heat inflows from the ambient air become comparable both with and without thermal insulation.

4. The dependence T_{surf} on the heat sink temperature T_{sink} is almost linear. This conclusion is true for all LHP orientations in the gravity field, with or without thermal insulation.

5. The most significant influence of the LHP orientation in gravity field is observed at $T_{\text{sink}} < 150^\circ\text{C}$. This is due to the fact that with Q_{evap} increasing, the mass flow rate of toluene in the LHP increases and the hydrostatic pressure drop becomes insignificant compared to pressure losses due to friction and local resistances.

Further implementation of cooling systems based on LHP in aircraft turbojet engines will be associated with the need to intensify heat transfer during heat rejection to the secondary air flow and with the analysis of the impact of vibration on LHP performances.

Contributions of authors: conceptualization, methodology – **Pavlo Gakal**; formulation of tasks, analysis – **Igor Rybalchenko**, **Oleksii Tretiak**; test bend design, software – **Viacheslav Nazarenko**; analysis of results – **Pavlo Gakal**, **Viacheslav Nazarenko**; writing

– original draft preparation, writing – review and editing – **Pavlo Gakal**.

Conflict of Interest

The authors declare that they have no conflict of interest in relation to this research, whether financial, personal, author ship or otherwise, that could affect the research and its results presented in this paper.

Financing

The research leading to these results has been funded and performed in the frame of the “*Aircraft Engine Valves Thermal Management with Advanced Loop Heat Pipe (EVAL)*” project. This project has received funding from the Clean Sky 2 Joint Undertaking under the European Union’s Horizon 2020 research and innovation program under Grant Agreement No 886615.

Data Availability

Data cannot be made available for reasons disclosed in the data availability statement.

Use of Artificial Intelligence

The authors confirm that they did not use artificial intelligence technologies when creating the current work.

Acknowledgements

The authors gratefully acknowledge the support provided by the members of the ALLATHERM Company, especially Dr. D. Mishkinis and Dr. I. Ušakovs for carrying out of the tests and for the fruitful discussions during preparation of this work.

All the authors have read and agreed to the published version of this manuscript.

References

- Li, W. J., Cheng, D. Y., Liu, X. G., Wang, Y. B., Shi, W. H., Tang, Z. X., Gao, F., Zeng, F. M., Chai, H. Y., Luo, W. B., Cong, Q., & Gao, Z. L. On-orbit service (OOS) of spacecraft: A review of engineering developments. *Progress in Aerospace Sciences*, 2019, vol. 108, pp. 32-120. DOI: 10.1016/j.paerosci.2019.01.004.
- Riehl, R. R., & Dutra, T. Development of an experimental loop heat pipe for application in future space missions. *Applied Thermal Engineering*, 2005, vol. 25, iss. 1, pp. 101-112. DOI: 10.1016/j.applthermaleng.2004.05.010.
- Phillips, A. L., & Wert, K. L. Loop Heat Pipe Anti-Icing System Development Program Summary. *SAE paper*, 2000, article no. 2000-01-2493. DOI: 10.4271/2000-01-2493.

4. Ghaffari, M. H. Feasibility Study on Designing a Flat Loop Heat Pipe (LHP) to Recover the Heat from Exhaust of a Gas Turbine. *World Academy of Science, Engineering and Technology International Journal of Mechanical and Mechatronic Engineering*, 2011, vol. 5, no. 12, pp. 2605-2608. DOI: 10.5281/zenodo.1334984.
5. Su, Q., Chang, S., Zhao, Y., & Dang, C. An experimental study on the heat transfer performance of a loop heat pipe system with ethanol-water mixture as working fluid for aircraft anti-icing. *International Journal of Heat and Mass Transfer*, 2019, no. 139, pp. 280-292. DOI: 10.1016/j.ijheatmasstransfer.2019.05.015.
6. Qian, S., Shinan, C., Yuanyuan, Z., Haikun, Z., & Chaobin, D. A review of loop heat pipes for aircraft anti-icing application. *Applied Thermal Engineering*, 2017, vol. 130, pp. 528-540. DOI: 10.1016/j.applthermaleng.2017.11.030.
7. Zhao, Y., Chang, S., Yang, B., Zhang, W., & Leng, M. Experimental study on the thermal performance of loop heat pipe for the aircraft anti-icing system. *International Journal of Heat and Mass Transfer*, 2017, no. 111, pp. 795-803. DOI: 10.1016/j.ijheatmasstransfer.2017.04.009.
8. van Heerden, A., Judt, D., Jafari, S., Lawson, C., Nikolaidis T., & Bosak, D. Aircraft thermal management: Practices, technology, system architectures. *Progress in Aerospace Sciences*, 2022, no. 128, DOI: 10.1016/j.paerosci.2021.100767.
9. Tecchio, C., Paiva, K. V., Oliveira, J. L. G., Mantelli, M. B. H., Gandolfi R., & Ribeiro, L. G. S. Passive cooling concept for onboard heat sources in aircrafts. *Experimental Thermal and Fluid Science*, 2017, no. 82, pp. 402-413. DOI: 10.1016/j.expthermflusc.2016.11.038.
10. Wang, H., Lin, G., Qin, H., Zhang R., Bai, L., & Guo, Y. Design and experimental validation of a high capacity loop heat pipe for avionics cooling. *Thermal Science and Engineering Progress*, 2023, no. 45, pp. 1-16. DOI: 10.1016/j.tsep.2023.102139.
11. Oliveira, J., Tecchio, C., Paiva, K., Mantelli, M., Gandolfi R., & Ribeiro, L. Passive aircraft cooling systems for variable thermal conditions. *Applied Thermal Engineering*, 2015, no. 79, pp. 88-97. DOI: 10.1016/j.applthermaleng.2015.01.021.
12. Zilio, C., Mancin, S., Hobot, R., Sarno, C., Pomme V., & Truffart, B. Loop Heat Pipe and mini-Vapour Cycle System for Helicopter Avionics Electronic Thermal Management. *Proceeding of the 16th International Refrigeration and Air Conditioning Conference*, Purdue, July 11-14, 2016. Available at <http://docs.lib.purdue.edu/iracc/1673>. (accessed 1.10.2024).
13. Anderson, W., Hartenstine, J., Ellis, M., Montgomery, J., & Peters, C. Electronics Cooling Using High Temperature Loop Heat Pipes With Multiple Condensers. *SAE Technical Paper*, 2010, article no. 2010-01-1736. DOI: 10.4271/2010-01-1736.
14. Mantelli, M. B. H., Almeida, J. C. P., & Mera, J. C. P. Experimental investigation of gravity and capillary assisted mini two-phase heat transfer loops for avionics. *International Journal of Thermal Sciences*, 2025, vol. 210. DOI: 10.1016/j.ijthermalsci.2024.109676. (accessed 1.10.2024).
15. Lawson, C. P., & Pointon, J. Thermal management of electromechanical actuation on an all-electric aircraft. *Proceeding of the 26th International Congress of Aeronautical*, 2008. Available at: http://icas.org/icas_archive/ICAS2008/PAPERS/243.pdf. (accessed 1.10.2024).
16. Donovan, M., & Del valle, P. Aeronautical Passive Energy Recovery System based on LHP Technology Extended Test Results. *SAE Technical Paper*, 2014, article no. 2014-01-2191. DOI: 10.4271/2014-01-2191.
17. Mishkinis, D., Usakovs, I., & Nasibulin, D. Experimental Study of Dual Evaporator LHP with Two Compensation Chambers. *Proceeding of the X International Seminar "Heat Pipes, Heat Pumps, Refrigerators, Power Sources"*, 2018. Available at: https://www.researchgate.net/publication/327729833_Experimental_Study_of_Dual_Evaporator_LHP_with_Two_Compensation_Chambers. (accessed 1.10.2024).
18. Gakal, P., Mishkinis, D., Leilands, A., Usakovs, I., Orlov, R., & Rogoviy, Y. Analysis of working fluids applicable for high-temperature. *IOP Conf. Ser.: Mater. Sci. Eng.*, 2022. DOI: 10.1088/1757-899X/1226/1/012036.

Received 30.10.2024, Accepted 21.01.2025

ЕКСПЕРИМЕНТАЛЬНЕ ДОСЛІДЖЕННЯ ХАРАКТЕРИСТИК СИСТЕМИ ОХОЛОДЖЕННЯ НА БАЗІ КОНТУРНОЇ ТЕПЛОВОЇ ТРУБИ ДЛЯ УМОВ ТУРБОРЕАКТИВНОГО ДВИГУНА З НАДВИСОКИМ СТУПЕНЕМ ДВОКОНТУРНОСТІ

*П. Г. Гакал, І. А. Рибальченко, О. В. Третяк,
В. В. Назаренко*

Предметом вивчення в статті є процеси теплопередачі в контурній тепловій трубі (КТТ) для вирішення прикладного завдання підтримання температурного режиму роботи клапанів системи відбору повітря

авіаційного двигуна. **Метою** є експериментальне обґрунтування працездатності та ефективності системи охолодження на базі КТТ для температурних умов перспективного авіаційного двигуна з надвисоким ступенем двоконтурності. **Завдання:** створити експериментальний стенд для дослідження процесів теплопередачі в системі охолодження на базі КТТ, який повинен відтворювати температурні умови роботи КТТ в складі авіаційного двигуна, орієнтацію КТТ в полі сили тяжіння. Дослідити працездатність системи охолодження для різного теплового навантаження, температури тепловідводу, орієнтації в полі сили тяжіння, додаткової теплоізоляції. Використовуваними **методами** є: експериментальний підхід, планування експерименту, статистичний метод обробки експериментальних результатів. Отримані такі **результати**. Створено експериментальний стенд для дослідження процесів теплопередачі в системі охолодження на базі КТТ, в якій в якості теплоносія використовується толуол. При створенні стенду враховано температурні умови роботи системи охолодження в складі перспективного авіаційного двигуна. Проведено дослідження працездатності системи охолодження при різних умовах орієнтації в полі сили тяжіння, температурі тепловідводу та різному тепловому навантаженні. В результаті отримані експериментальні результати, які дозволили провести аналіз впливу орієнтації системи охолодження в полі сили тяжіння, температури тепловідводу, додаткової вакуумної теплоізоляції випарника та рідинної магістралі КТТ та її працездатність та ефективність. **Висновки.** Новизна отриманих результатів полягає в наступному: вперше експериментально обґрунтовано можливість використання системи охолодження на базі КТТ в температурних умовах, характерних для перспективного авіаційного двигуна з надвисоким ступенем двоконтурності; доведено, що КТТ з толуолом в якості теплоносія в складі системи охолодження може ефективно працювати стабільно, без пульсацій та без перегріву охолоджуваних приладів при різному температурному навантаженні, температурі тепловідводу та орієнтації в полі сили тяжіння.

Ключові слова: система охолодження; контурна тепла труба; теплопередача; турбореактивний двигун з надвисоким ступенем двоконтурності; споживання палива.

Гакал Павло Григорович – д-р техн. наук, доц., проф. каф. аерокосмічної теплотехніки, Національний аерокосмічний університет ім. М. С. Жуковського «Харківський авіаційний інститут», Харків, Україна.

Рибальченко Ігор Анатольович – начальник міжнародного відділу міжнародних проєктів та програм, Національний аерокосмічний університет ім. М. С. Жуковського «Харківський авіаційний інститут», Харків, Україна.

Третяк Олексій Володимирович – д-р техн. наук, доц., зав. каф. аерогідродинаміки, Національний аерокосмічний університет ім. М. С. Жуковського «Харківський авіаційний інститут», Харків, Україна.

Назаренко Вячеслав Вікторович – асп. каф. аерогідродинаміки, Національний аерокосмічний університет ім. М. С. Жуковського «Харківський авіаційний інститут», Харків, Україна.

Pavlo Gakal – Doctor of Technical Science, Associate Professor, Professor at the Aerospace Thermal Engineering Department, National Aerospace University "Kharkiv Aviation Institute", Kharkiv, Ukraine, e-mail: p.gakal@khai.edu. ORCID: 0000-0003-3043-2448, ResearchGate: Pavlo-Gakal.

Igor Rybalchenko – Head of International STI Project Office, National Aerospace University "Kharkiv Aviation Institute", Kharkiv, Ukraine, e-mail: i.rybalchenko@khai.edu.

Oleksii Tretyak – Doctor of Technical Science, Associate Professor, Head of the Department of Aerohydrodynamics, National Aerospace University "Kharkiv Aviation Institute", Kharkiv, Ukraine, e-mail: o.tretyak@khai.edu, ORCID: 0000-0002-7295-5784, ResearchGate: Oleksii-Tretiak-2.

Viacheslav Nazarenko – PhD Student, National Aerospace University "Kharkiv Aviation Institute", Kharkiv, Ukraine, e-mail: v.v.nazarenko@khai.edu. ORCID: 0009-0000-8154-9131, ResearchGate: Viacheslav-Nazarenko.